Skin Melanoma Classification from Dermoscopy Images using ANU-Net Technique

Vankayalapati Radhika, Dr. B. Sai Chandana
School of Computer Science Engineering, VIT-AP University, Amaravati, Andhra Pradesh, India

***Abstract*—Cells in any area of the body might develop cancer when they begin to grow uncontrollably. Other body regions may become affected by it. Skin cancer known as melanoma develops when melanocytes, or cells that create melanin, the pigment that gives skin its appearance of color, start to develop out of control. Melanoma is deadly because, if not caught early and addressed, it has a high propensity to spread to other regions of the body. Analyzing digital dermoscopy images, create a unique approach to categorizing melanocytic tumors as malignant or benign. Every single newly formed mole has a unique shape and colour compared to the pre-existing moles and given few more issues to classify the melanoma. To overcome all of these issues, this paper uses deep learning techniques. In this paper, a four-step system for classifying melanoma is described. The first stage is pre-processing, followed by the removal of hair from dermoscopic images using a Laplacian-based algorithm and then removing noise from the images using a Median filter. The second method is feature extraction from pre-processed images. Extracting features including texture, shape, and color using the Principal Component Analysis (PCA) technique. Thirdly, the LeNet-5 approach is utilized to locate the lesion location and segment the skin lesion. Fourth, the ANU-Net technique is used to categorize the lesion as cancerous (melanoma) or non-cancerous (non-melanoma). Evaluated based on performance parameters such as precision, sensitivity, accuracy, and specificity. Results are compared to those of current systems and show higher accuracy.**

***Keywords*—Melanoma; LeNet-5; ANU-Net; dermoscopy images; benign; classification**

I. Introduction

Melanoma is a prevalent form of malignant that develops in the epidermal layer of the skin from abnormal cells caused by exposure to UV light. In an area with intense sunlight, one in five Americans (US) is at risk of developing skin cancer. Melanoma is the nineteenth most prevalent malignancy overall among all forms of skin cancer, with around 3.0 million new cases reported in 2018 [1]. In the US alone in 2019, melanoma claimed the lives of 2,490 females and 4,740 males on average. In 2020, there will likely be 1.0 million new cases of melanoma, according to projections. 2020 is expected to see an estimated 6,850 additional cases of melanoma deaths in the US alone, with 2,240 females and 4,610 males [2]. Skin cancer is currently diagnosed using a variety of imaging methods, including dermoscopic images, magnetic resonance imaging, optical coherence tomography, and confocal scanning laser microscopy. Dermatologists examine those images visually, which is frequently a laborious and time-consuming operation.

Melanoma is the worst type of cancer among skin cancers, and its prevalence is rising quickly globally. Early detection is crucial since skin cancer can be treated with a straightforward excision. Most of the time, the visual analysis could be inappropriate and result in a false identification because the different skin lesions (non-melanoma and melanoma) are similar to one another [3-5]. A non-invasive skin imaging procedure called dermoscopy enables a magnified view of the skin's surface and subdermal processes. By aiding in the early detection of MM, dermoscopy images have significantly increased the survival rate of patients. While still the undisputed top standard, expert human diagnoses are nevertheless prone to bias.

The number of skin cancer diagnoses is increasing in past years. Melanoma and benign skin cancer are the two main varieties. Melanoma is one of the worst forms of skin cancer and is a major cause of death in young people each year [6, 7]. The severity and symptoms of skin disorders vary; for instance, a nevus is a normal skin lesion caused by the growth of pigment-producing cells also known as melanocytes, but melanoma is a severe form of skin cancer that can arise from a benign lesion [8].

The same nevus cells that produce pigment can give rise to melanoma. Melanoma is a fast-evolving disease that is responsible for a high death rate among the global population, according to research in both the medical and analytical fields [9-11]. With the early-stage discovery, the skin lesion can be treated. If melanoma is detected early, the survival percentage will be higher and it will be treatable. However, the manual diagnosing process necessitates dermatology specialists with appropriate training. An experienced dermatologist is very expensive and takes a lot of time. The most important phase in these systems is feature extraction, where several features can be utilized to check the pigmentation, shape, or evolution of skin lesions or to distinguish melanomas from benign lesions [12]. These features include asymmetry, border irregularity, and color. Dermoscopy technology offers a further improvement in diagnosis. Applying the dermoscopy approach to the skin will allow you to highlight locations by taking illuminated, magnified images of the skin lesion without making any incisions. Additionally, if the skin surface reflection is eliminated, the visual impact of the deeper skin layer can be enhanced. However, due to a variety of problems, classifying melanoma dermoscopy images is a challenging task [13]. In this paper, proposed four steps to classify the melanoma. They are pre-processing, feature extraction, segmentation, and classification. Initially, utilize a Laplacian-based algorithm to remove hair from dermoscopic images

during the pre-processing stage, and then a Median filter to eliminate noise to segment the dermoscopic images. The principal component analysis method is used for feature extraction to extract features including texture, shape, and color. After feature extraction completed, the skin lesion is segmented using the LeNet-5 technique to identify the lesion region, and the classification process is then carried out. Using the ANU-Net approach, categorize the lesion into benign (non-melanoma) and malignant (melanoma) during the classification stage. The key contribution of this paper is:

- This paper uses deep learning techniques for classifying melanoma into malignant and benign by using dermoscopic images. First, do pre-processing to remove hairs on images to get better segmentation and also remove noise on images.
- A PCA method using for feature extraction process to obtain the features such as shape, color, and texture of the image.
- Then utilizing LeNet-5 technique for segment the skin lesion area in dermoscopic images and after that classify the skin lesion into non-melanoma or melanoma using ANU-Net technique. Here collect dermoscopic images from ISIC 2020 dataset.

This paper is structured as follows. The related research on deep learning-based melanoma classification is covered in Section II. The proposed methodology and its components are covered in detail in Section III. The experimental strategy is described in Section IV. The study is reviewed in Section V along with suggestions for additional research.

II. Literature Survey

A literature review is presented and discussed in this paper to offer a speculative background about melanoma skin cancer classification. Hosny et al. [14] suggested a classification method based on DCNN. There are three primary steps in the suggested procedure. In the beginning, the ROI is segmented in the input color skin images during preprocessing. Second, translation transformations and rotation are used to enhance the segmented ROI images. Third, various deep convolutional neural network (DCNN) designs are used, including GoogleNet, Alex-net, and ResNet101. To better suit the task of classifying lesions, the final three layers are removed and replaced with fresh ones. DermIS & DermQuest, MED-NODE, and ISIC 2017 are three separate datasets that were used to assess the performance of the suggested technique.

To detect and categorize dangerous skin lesions (melanoma type), Ponomaryov et al. [15] introduced a computer-aided detection (CAD) system that combines handcrafted features from the medical algorithm Asymmetry Borders-Colors-Dermatoscopic Structures (ABCD) rule with DL features using Mutual Information (MI) measurements. Pre-processing, extraction of features, feature fusion, and categorization are the steps in a CAD system that may be distilled into a single phrase. To identify the Region of Interest (ROI), a lesion image is improved, segmented, and filtered during the preprocessing stage. The feature extraction method is then carried out. Shape, color, and texture are examples of handcrafted features that are utilized to represent the ABCD rule. DL features are obtained using a CNN framework that has been pre-trained on ILSVRC ImageNet. Utilizing MI denotes a fusion rule, the most crucial data from both kinds of characteristics are gathered. Finally, numerous techniques are used during the classification process, including Relevant Vector Machines (RVMs), Linear Regression (LR), and Support Vector Machines (SVMs). The public dataset from ISIC 2018 was used to evaluate the developed system.

An excellent and efficient melanoma detection approach was presented by Masood et al. [16]. Three steps make up the suggested approach: 1) image preprocessing, 2) use of a Faster-RCNN for skin cancer localization, and 3) application of an SVM for the categorization of customized skin cancer regions into malignant and benign classes. The suggested technique's effectiveness is assessed utilizing data from the benchmark ISIC-2016 dataset, which was made available by the ISBI Challenge 2016. This dataset is diverse in terms of differences in color, luminescence, melanoma size, and texture, as well as the noise presence, blurring, small blood vessels, and hairs, among other things. Additionally, they validated the technique across multiple datasets using the ISIC-2017 dataset to demonstrate its effectiveness in practical settings.

The Automated Skin-Melanoma Detection (ASMD) system with Melanoma-Index (MI) was presented by Tang et al. [17] as being unique and original. The system includes binary classification, entropy, and energy feature mining, image pre-processing, Bi-Dimensional Empirical Mode Decomposition (BEMD), and image texture improvement. The system's design was influenced by feature ranking, and the quality of the system was evaluated using Student's t-test and other statistical techniques. Using benchmark databases, the proposed ASMD was applied to 600 DD malignant and 600 benign images.

Four steps are included in the Kumar et al. [18] proposed system for melanoma identification and categorization: pre-processing, which includes dermoscopic images being resized, and noise and hair being eliminated; image segmentation, which involves locating the site of the lesion; extraction of feature, which involves obtaining features from the segmented lesion and then categorization; and classifying the lesion as benign or malignant. To produce skin lesions, a modified GrabCut algorithm is used. Using machine learning techniques like ANN, k-NN, SVM, and logistic regression, segmented lesions are categorized, and their performance is assessed in terms of specificity, accuracy, and sensitivity.

Rahman et al. [19] introduced an automated approach for pixel-based seed-segmented images with multilevel and fusion characteristics downsizing for the recognition and detection of skin lesions. The suggested approach entails four crucial steps: Implemented methods include: (a) mean-based function feeding input to bottom-hat and top-hat filters that were later fused for contrast increasing; (b) graph-cut method-based lesion segmentation and seed region growing and fusing both segmented lesions through pixel-based fusion; (c) simple concatenation and multilevel feature extraction; The method's effectiveness is tested in two independent experiments.

From the literature survey, some of common problems are noticed. They are, every single newly generated mole differs from the pre-existing moles in terms of shape and colour. The mole's outline or outer covering is uneven, largely asymmetrical, and appears gritty. It states that around half of the moles present do not match the other half of the moles. Accurately determining the importance of a specific feature is challenging. For effective medical image diagnosis, a collection of more sophisticated deep-learning architectures should be used. To overcome these issues this paper used effective recent proposed methodologies to classify the melanoma clearly.

III. Proposed Methodology

The most dangerous type of skin cancer, melanoma is on the rise all over the world. Melanoma incidence has increased globally during the past ten years. The proposed methodology has four steps: Pre-processing, Feature Extraction, Segmentation, and Classification. And every step is evaluated below. Initially, pre-processing for removing hair from the dermoscopic images using the Laplacian-based algorithm, and then removing noise from the images using the Median filter. In addition, feature extraction from pre-processed images using the Principal Component Analysis (PCA) approach for extracting the characteristics like texture, shape, and color. Furthermore, the segmentation process for identifying the lesion area and segmenting skin lesion using the LeNet-5 technique, and then, classification; here categorizing lesion as benign and malignant using the ANU-Net method. It is classified into benign (non-melanoma) and malignant (melanoma).

The complete performance of the melanoma classification process is displayed in Fig. 1.

A. Pre-processing

In pre-processing step, remove the hair from input images and then denoise the images for better segmentation of melanoma. Initially, remove the hair from dermoscopic input images because some melanoma is significantly or partially obscured by body hairs using Laplacian-based algorithm to every image. A sharpening filter based on the Laplace operator is applied to the image is made grayscale. Then the original input image is seperate from the filtered image. It employs a 3x3 Wiener filter adaptive noise removal to eliminate any potential noise. After hair removal done, here remove noise from dermoscopic images.

Such noise is removed from dermoscopic images using the median filter, which uses a weighted average sum of the nearest pixels. The median filter performs well in terms of maintaining an image's edges. After hair removal, images are given to a median filter to eliminate noise. Fig. 2 illustrates the effectiveness of the noise and hair removal processes during the pre-processing stage.

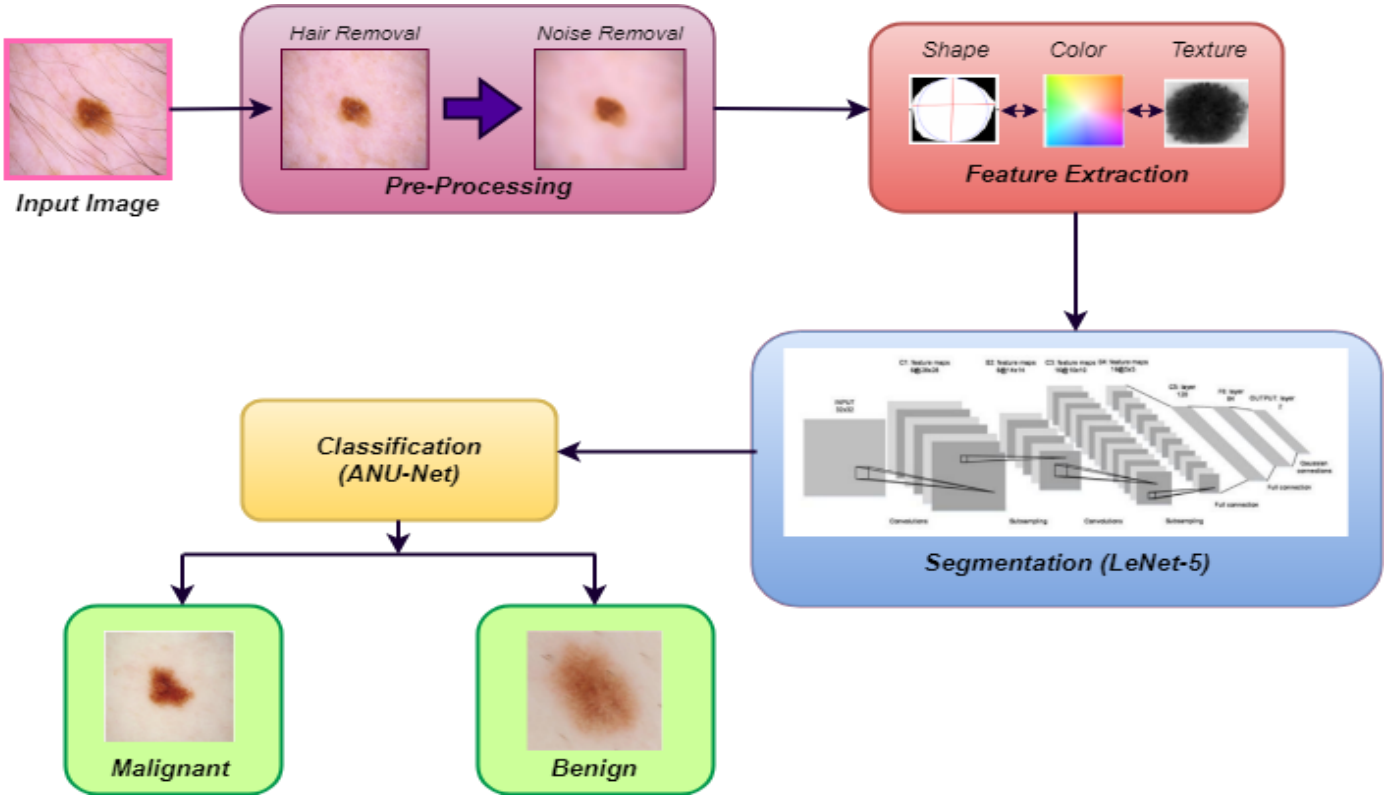

Fig. 1. The Proposed Architecture for Melanoma Classification.

Fig. 2. Process of Hair Remove and Noise Removal in Pre-processing Step.

B. Feature Extraction

After pre-processing, the characteristics that would be useful in features of the images are extracted using feature extraction techniques. For better prediction of melanoma from dermoscopic images, features like shape, color, and texture should be extracted. In this step, the features were extracted by using Principal Component Analysis (PCA). The obtaining of features is a significant phase in the model construction process. A system can be built using a variety of features, including color, shape, and texture, as well as SURF (speeded-up robust features). The PCA method is utilized to increase explainable while simultaneously reducing the loss of details to reduce the dimension of the dataset being used. The goal of PCA, a mathematical approach that uses a principal component examination, is to reduce the dataset dimension. An orthogonal linear transformation is another name for the process of transforming data into a new coordinate system. With the aid of linear combinations, the native features show new features. The traits with increasing variance are appropriate for dispatching. Accordingly, the PCA method converts the n vectors x_1,x_2,….,x_n from the d-dimensional space to the n vectors x_1,x_2,….,x_n in a new d-dimensional space.

$$x'i = \sum k = 1d'ak, iek, d' \leq d, \tag{1}$$

Where, d' is a space with n dimensions, n vectors, and ek eigenvectors that are the greatest eigenvectors for ak, i are the projections of the original vector $x'i$ and scatter matrix S on the eigenvector ek.

In PCA, Single Value Decay (SVD) is typically established on the input data matrix. Based on the optimization algorithm, a PCA technique may be developed. During the optimization process, the data reconstruction error and variance maximization of the projected input data can be examined.

$\overline{\overline{W_i}} \in S^n, i = 1,2,3....o, o < n$ information variance can be estimated in the orthonormal direction with a constrained amount of options using PCA to determine the orthonormal direction O in a given space. Without losing any data in the resulting structure of dimension $d \in S^n$, the input vector is translated into O-dimensional space. In the input data, which consists of vector d, the O-Dimension is projected using $\overline{\overline{W}}$, where the inner product $(d^t \overline{\overline{Wi}})$ is obtained and the misplaced outcome dimension is obtained. Since PCA calculates unit directions, the information can be anticipated into the input vector. Where Y = $d^t \overline{\overline{Wi}}$, it has a large variance and is signified by greater variance. It will be written as:

$$\sigma_{PCA}(W) = \sigma\left[y^2\right] = d^T C\overline{\overline{W_i}} = \frac{W^I CW}{\left\|W\right\|^2} \tag{2}$$

where $\overline{\overline{W}}$ =W/||W||

Apply the estimation in the linear square estimation after reconstructing the input data, or $\hat{d}$.

$$\hat{d}_t = \sum_{i=1}^{O} g_{i(t)\overline{\overline{W_i}}} \tag{3}$$

With the use of data reconstruction, the error can be recreated and identified by comparing the differences between the original and corrected data.

$$\text{e=d-}\hat{d}_t = \sum_{i=O+1}^{n} a_i \overline{\overline{W_i}} \tag{4}$$

To predict this issue, implement a novel method for dimension restricting and increasing the entertainment of PCA following in overall presentation development. Based on PCA, the reconstruction error can be reduced. When extending k-dimensional data to subspace, calculations are visible.

$$PCA\ reconstruction = PC\ scores. Eigenvectors\ T + Mean$$

Based on the proposed technique, a maximum likelihood-based model may be used to map the underlying space into the data space.

$$x = \varepsilon + \mu + \int \Lambda \tag{5}$$

In a linear transformation, the variable $(p * 1)$ is designated as the variable, x is denoted as the high-dimensional factor and is also defined as $(p \times O), f\ is\ (O \times 1), \Lambda \to x,\ \mu(p \times 1)$ is defined as the mean vector, and ε is defined as Gaussian random error, the $\mu(p \times 1)$ denoted as the input signal vector of noise. The feasible result's input vector is represented by

$$p\left(\varepsilon; \sigma^2\right) = \left(2\pi\sigma^2\right)^{\frac{-p}{2}} \exp\left(\frac{-1}{2}\varepsilon'\varepsilon\right) \tag{6}$$

It will increase by the conditional probability of

$$p\left(x/f;\Lambda,\mu,\sigma^2\right)=\left(2\pi\sigma^2\right)^{-\frac{p}{2}}\exp\left(-\frac{1}{2}\|x-\mu-f\Lambda\|^2\right) \quad (7)$$

The dataset of the absolute distribution of a specific space is delivered by such a model without changing any errors or data that were not distributed for the specified probabilistic limit. The PCA model's primary goal can be achieved by fully revealing unknown parameters like Λ and μ, maximum noise variance σ^2-based likelihood observations.

$$L\left(\Lambda,\mu,\sigma^2\mid x\right)$$

$$(2\pi)^{-\frac{np}{2}}|\sum|^{-\frac{n}{2}}\exp\left[-\frac{1}{2}\sum_{i=1}^{n}(x_i-\mu)'\sum^{-1}(x_i-\mu)\right]$$

$$\left(x_i-\mu)'\sum^{-1}\right)(x_i-\mu) \quad (8)$$

Another way to express maximum likelihood observation is in $tr\left(\sum^{-1}S\right)$ where S is a possible expression,

$$S=\frac{1}{n}\sum_{i=1}^{n}(x_i-\hat{\mu})(x_i-\hat{\mu})' \quad (9)$$

The maximum log-likelihood can be expressed using the equation below.

$$L\left(\Lambda,\mu,\sigma^2\mid x\right)=-\frac{np}{2}\log(2\pi)-\frac{n}{2}\log|\sum|-\frac{n}{2}tr\left[\sum^{-1}S\right] \quad (10)$$

Based on PCA's data reconstruction, Λ and σ^2 the error can be minimized while still producing a superior answer. The highest possible possibility of σ^2.

$$\hat{\sigma}^2ML=\sum_{j=m+1}^{p}\lambda_j\times\frac{1}{p-m} \quad (11)$$

Effective parameters are reduced in the feature reconstruction process by applying the maximum likelihood model, which is based on the above-mentioned model's decreased error and increased production in feature extraction based on PCA. The PCA method giving significant results as expected and extract the feature of melanoma or benign dermoscopic images well. The major benefit of PCA for index generation over traditional techniques is that it does not assign arbitrary and subjective weights to various indicators. The results of a multivariate statistical analysis of a few chosen indicators are used to determine the weights allocation in PCA for the construction of the index. The principal component analysis method extracted the features such as shape, color, and texture very well. And this method work better to feature extraction without any issues.

C. Segmentation

Following feature extraction, the image segmentation procedure separates the scene into the background and foreground. After extracted the features from dermoscopic images, at next step need to segment the issue part from images. Because segmentation of issue part is more important to predict that if it's melanoma or not. In this research, the segmentation process was carried out using LeNet-5 technique. When the background and foreground colors of an image are highly similar, the LeNet-5 method is used. Because the other technique's results are unsuccessful. Below is a description of the LeNet-5 method.

Using this segmentation network, the effective deep skin lesions are divided into groups. Many other CNN types can be used for segmentation depending on the objectives of the application, and the melanoma was segmented using a LeNet-5 pre-trained network. An input layer, two pooling levels, one fully connected layer, two convolutional layers, and an output layer made up a total of seven layers in LeNet-5 [21]. Table I displays the precise design of the LeNet-5. LeNet-5's weighted layers are constructed using the idea of removing convolution layer blocks by utilizing shortcut connections. The "bottleneck" blocks, which are the fundamental construction blocks, follow two design principles: The same amount of filters are used to create the same output feature size. The convolution layers down-sample at a rate of two strides per layer. Batch normalization is carried out both before and after each convolution and before the rectified linear unit (ReLU) is activated.

An identity shortcut is used when the input and output dimensions are identical. The projection shortcut utilising 1x1 convolutions is used to match the dimensions when the dimensions are enhanced. The segment of the skin lesion region is transmitted to the classification and RPN networks from the last convolutional layer. In the LeNet-5 segmentation network, only the 49 convolutional layers are utilized; fully connected and average pooling layers are not. Because only the segmentation network, not the final classification is required by the RPN and classification network.

These region proposals are used by the final segmentation network to classify objects. In the RPN, anchor boxes with various scales and aspect ratios are first formed across each pixel of the feature map. Usually, nine anchor boxes with aspect ratios of 1:1, 1:2, and 2:1 and scales of 128, 256, and 512 are used. RPN forecasts the likelihood that a backdrop or item will appear in an anchor box. The necessary object proposals are forwarded to the following stage as a list of filtered anchor boxes. To convert the final anticipated region proposals from the anchor boxes, apply Eq. (12) and (13). Equation illustrates the scale-invariant translation between the center coordinates (12). The height and width are translated into log space using equation (13).

$$V_x=\frac{x_p-x_a}{w_a},V_y=\frac{y_p-y_a}{h_a} \quad (12)$$

$$V_w=\log\left(\frac{w_p}{w_a}\right),V_h=\log\left(\frac{h_p}{h_a}\right) \quad (13)$$

TABLE I. LENET-5 SEGMENTATION NETWORK

Layers	Name of the Layers	Input size	Output size	Pooled area	Convolution kernel size	Step size
Input	Input layer	32*32	28*28		5*5	1
Layer1	Convolutional layers	6@28*28	6@14*14	2*2		2
Layer 2	Pooled layers	6@14*14	16@10*10		5*5	1
Layer 3	Convolutional layers	16@10*10	16@5*5	2*2		2
Layer 4	Pooled layers	16@5*5	120@1*1		5*5	1
Layer 5	Fully connected layer	1*120	1*84			
Layer 6	Fully connected layer	1*84	1*7			
Output	Output layer	1*7				

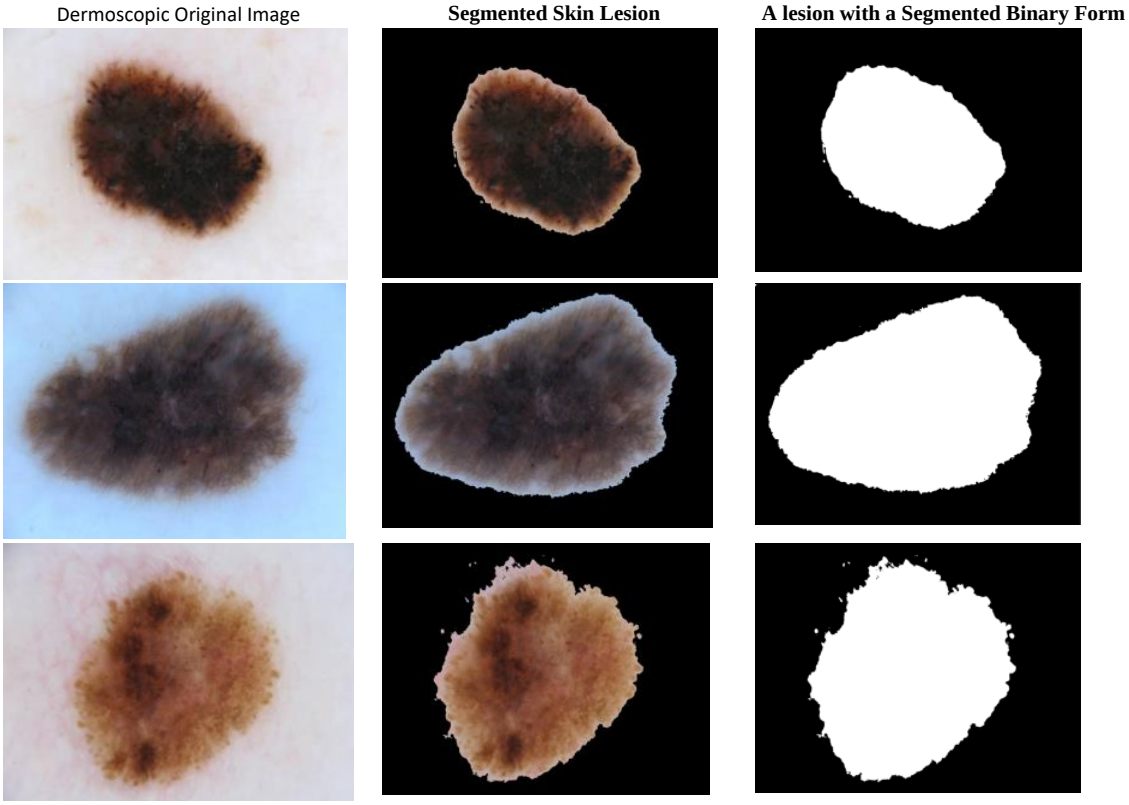

Fig. 3. Sample Segmentation Performance using the LeNet-5 Technique.

Where the bounding box regression vectors are represented by V_x V_y V_w, and V_h, and coordinates for the height, width, and center in x and y are depicted by *h*, *w*, and *x*, *y*. Additionally, x_a x_p are the corresponding centers of the anchor and proposal box. The convolutional layers and fully connected layers of LeNet-5 technique are utilized in segmentation step to segment the melanoma issue part in dermoscopic images based on extracted features. The LeNet-5 method segments the skin lesion area accurately.

Some of the sample processes of segmentation of skin lesion performance are shown in above Fig. 3. It shows the segmented skin lesion area from dermoscopic images and also given the binary form of segmented skin lesion area using segmented technique LeNet-5.

D. Classification of Benign and Malignant

In the classification step, classify the segmented skin lesion into malignant or benign using the ANU-Net technique. It uses the skin lesion from segmented images for classifying whether the issue part is melanoma or not. Images with closely matched foreground and background colors are used with the ANU-Net technique. The ANU-Net technique is described below.

Develop an integrated network called Attention U-Net++ for medical image classification. Using nested U-Net architecture, which takes it from DenseNet, a series of U-Nets with different depths are integrated. In contrast to U-Net, which used nested convolutional blocks and constructed dense skip links between the decoder and encoder at various levels, the nested Framework makes use of convolutional blocks that are layered within each other [20]. Every nested convolutional

block in layered U-Nets employs numerous convolution layers to gather semantic data. The concatenation layer can integrate semantic data from different levels since each layer in the block is connected via connections. The following are some benefits of the new nested design:

- Layered architecture may avoid the time-consuming procedure of choosing deep and shallow features by assessing the value of features at various depths on its own.
- Only an encoder must be trained because the feature extractor is shared by all of the U-Nets in a nested arrangement.
- Since different decoder paths independently restore distinct layers of features, they can collect hierarchical decoded masks from a variety of levels in tiered architecture.

1) Attention Gate (AG): Attention Gate employs the PASSR net's model and includes an effective AG into nested architecture.

The AG feature selection Phase is described as follows:

$$F = \sigma_1[(W_f^T \times f + b_f) + (W_g^T \times g + b_g)] \tag{14}$$

$$\alpha = \sigma_2(W_\theta^T \times F + b_\theta) \tag{15}$$

$$output = f \times \alpha \tag{16}$$

The effective function of the Attention Gate allows it to classify the task-related target region more effectively while suppressing the task-unrelated target region. In research, Attention Gate is used to enhance the capability of semantic data propagation across skip links in the creatively recommended network.

2) Attention-based nested U-Net: The ANU-Net is a network that is integrated for classifying medical images and is based on the Attention mechanism and Nested U-Net architecture. In the ANU-Net, which utilizes nested U-Net as its main network architecture. Then, additional helpful hierarchical characteristics can be retrieved. The encoder sends the context data it has gathered to the appropriate layers' decoder via the wide skip connections.

For each convolutional block, the decoder receives two equivalent image features when there are multiple dense skip connections: The preliminary feature maps are produced by earlier Attention Gates with residual connections at the same depth, while the final feature map is produced by a deeper block deconvolution procedure. The decoder reconstructs features starting at the bottom and adding up all received feature maps.

The extracted feature map from ANU-Net may be expressed as follows: Let $X_{i,j}$ indicate the outcome of the convolutional block, while the feature depth is denoted as i and the convolution block's sequence as j.

$$X_{i,j} = \begin{cases} \Phi[X_{i-1,j}] & , j = 0 \\ \Phi[\sum_{k=0}^{j=1} Ag(X_{i,k}), Up(X_{i+1,j-1})] & , j > 0 \end{cases} \tag{17}$$

$Up(X_{i+1,j-1})$ and $Ag(X_{i,k})$ the attention gate and mean up-sampling selection accordingly, $\sum_{k=0}^{j=1} Ag(X_{i,k})$ indicate that concatenate the outcome of the AG from node X_i, k=0 to X_i, k= j−1 in the i^{th} layer.

After the concatenation operation, the decoder's convolution blocks will only employ the encoder's chosen same-scale feature maps rather than all of the feature maps that were acquired via dense skip connections. This layer's output from the j previous blocks acts as an input, while the second layer's up-sampling function of block X1 provides additional input. The network transfer of features gathered by the encoder is one of two significant ANU-Net innovations. Furthermore, Attention Gate is used in the decoder path between layered blocks that are recovered at different layers and can be connected with a specific choice. As a result, ANU-Net accuracy ought to be raised. The proposed classification technique works well and classify the dermoscopic image as malignant or benign. The ANU-Net techniques improved the time complicity of classification and given better classification accuracy.

IV. Results and Discussion

This section's compares the approach to "state-of-the-art" techniques by categorizing melanoma using the dataset's analysis and technique for extracting features from skin lesions. Given are the assessment findings based on experimental data in the following subsections to evaluate methodology.

A. Dataset Description

There are 33,126 dermoscopic images of benign and malignant skin lesions in the ISIC-2020 dataset, with a high percentage of benign lesions. Only 584 of the 33,126 skin lesion images were classified as malignant melanoma. The primary factor that led to the selection of this dataset above others was the fact that the skin lesions are discernible and are not masked by any artifacts. Furthermore, the skin lesions' micro-features are distinct and easy to see. The efficiency of feature extraction is improved by this. The dataset sample images are seen in Fig. 4.

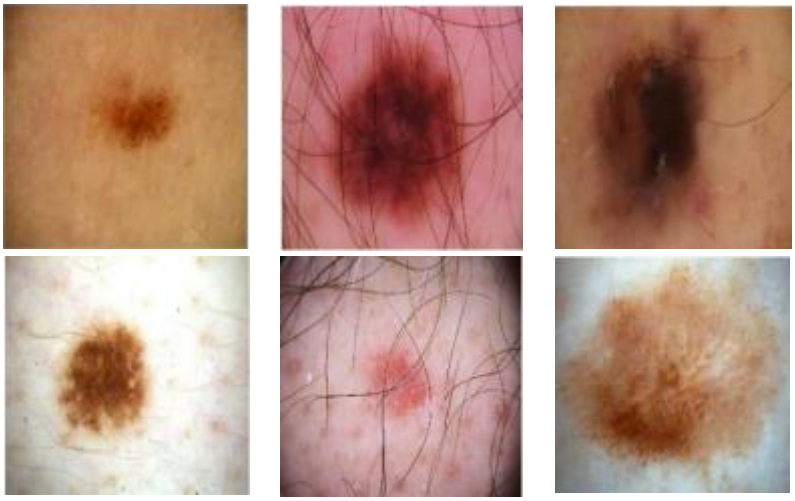

Fig. 4. Shows Various Images of Skin Lesions in the Dataset.

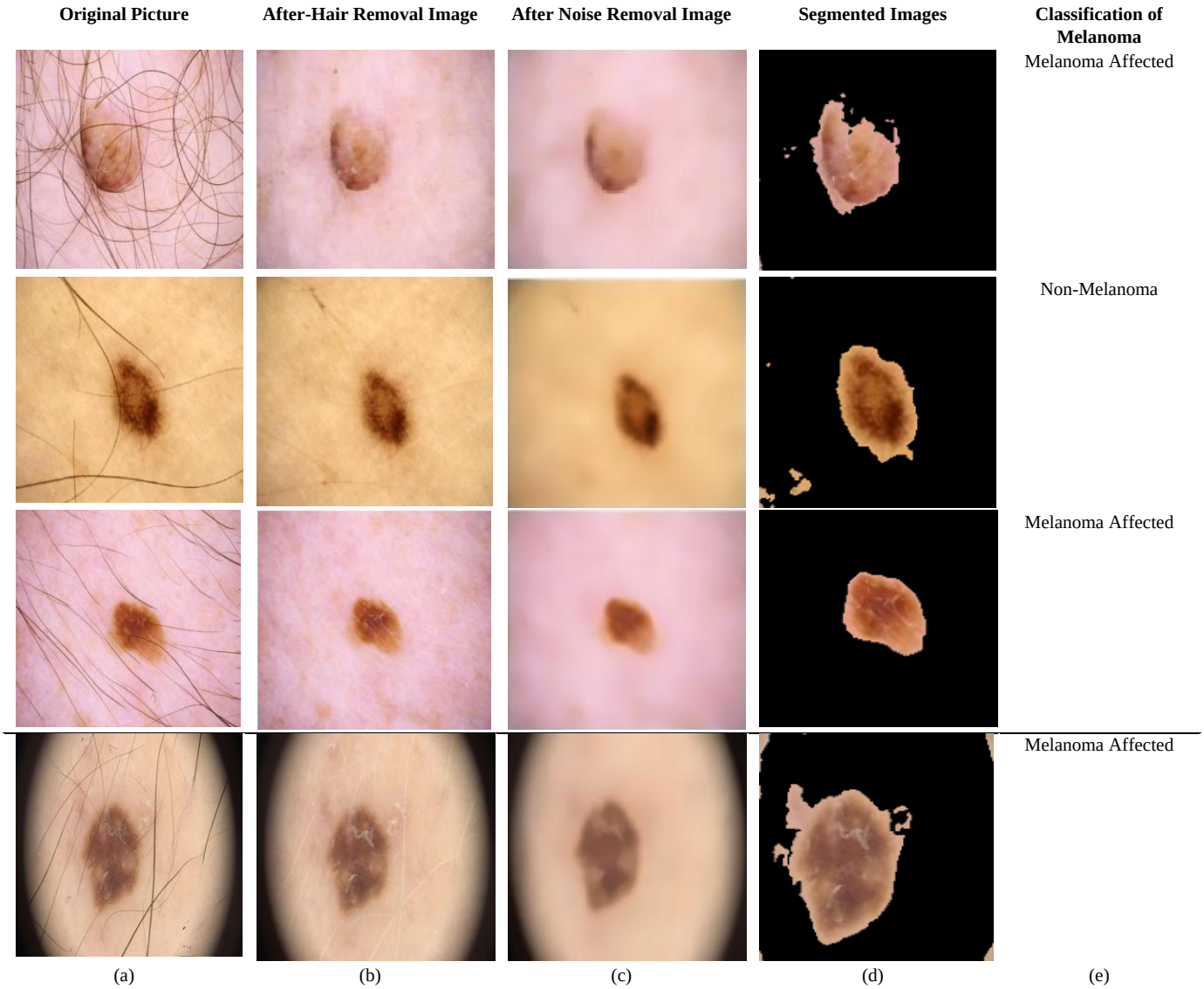

Fig. 5. The Experimental Outputs: (a) Original Image, (b) After Hair Removal Image, (c) After Noise Removal Image, (d) Segmented Images, (e) Classification of Melanoma.

B. Quantitative Metrics

The performance of the proposed method for classifying the skin lesion into malignant or benign is to give a better result. Here, first, are given an input dermoscopic image from ISIC 2020 dataset. For a better segmentation process, remove the hair from input dermoscopic images and then the noise from this input image in pre-processing step. Segment the skin lesion portion from the dermoscopic image using LeNet-5 technique. It determines the skin lesion's malignant (melanoma) or benign (benign) status using this segmented image (non-melanoma) utilizing the classification technique ANU-Net. The experiment performed well and produced superior results. The findings of the experiment are displayed in Fig. 5.

C. Evaluation Metrics

In terms of performance measures, looked at the proposed method's Accuracy (A), Precision (P), F1-score (F), and Recall (R). These metrics indicate:

Accuracy

The percentage of samples that were correctly identified relative to all samples is known as accuracy. In general, a classifier performs better the higher accuracy. Eq. (18) illustrates the meaning of accuracy.

$$Accuracy = \frac{TP+TN}{TP+FN+FP+TN} \quad (18)$$

Sensitivity

Sensitivity, also known as recall, measures how well a classifier can identify positive samples by representing the percentage of all positive samples that are predicted. Eq. (19) defines sensitivity.

$$Sensitivity = \frac{TP}{TP+FN} \quad (19)$$

Specificity

Specificity measures the classifier's capacity to identify negative samples by representing the percentage of all negative samples that are successfully classified. Eq. (20) illustrates the definition of specificity.

$$Specificity = \frac{TN}{TN+FP} \quad (20)$$

Precision

Precision is defined as the ratio of precisely anticipated positive occurrences to all anticipated positive observations. Precision is the capacity to do the following things:

$$Precision = \frac{TP}{TP+FP} \quad (21)$$

D. Performance Evaluation

In experimental performance, the proposed technique has the highest classification accuracy compared with other existing techniques. Table II shows the results for DenseNet-121, ResNet-50, Inceptionv3, and the proposed ANU-Net on the ISIC 2020 dataset in terms of accuracy, specificity, sensitivity, and Precision. Based on the results, the proposed methodology has higher classification accuracy values than other existing approaches. It is consistent with the experimental findings for the melanoma classification into two types, malignant and benign. By using the proposed ANU-Net classification technique, the time complexity is reduced, effective training is performed, and the overall performance of the classification is improved compared with other existing techniques.

Here, for comparison three other existing methods are chosen to compare with the proposed technique. Compared with other techniques, the proposed methodology gives high accuracy values for classification. In Table II, the classification accuracy achieved 98.78% utilizing the proposed methodology ANU-Net technique compared with other techniques DenseNet-121 has 93.65%, ResNet-50 has 96.96%, and Inceptionsv3 has 97.17%. The proposed methodology provide effective outcomes and the classification accuracy is higher than others. Additionally, when compared to other existing methodologies, DenseNet-121 has the lowest accuracy rate at 93.65%. This accuracy comparison model is shown in Fig. 6.

In Table II, the sensitivity metric achieved 98.39% using the proposed method ANU-Net technique compared with other techniques DenseNet-121 has 95.83%, ResNet-50 has 96.53%, and Inceptionsv3 has 96.32%. This sensitivity comparison model is shown in Fig. 7.

TABLE II. THE PERFORMANCE OF CLASSIFICATION TECHNIQUE

Models	Accuracy	Sensitivity	Specificity	Precision
DenseNet-121	93.65	95.83	93.48	96.13
ResNet-50	96.96	96.53	96.53	95.32
Inceptionv3	97.17	96.32	96.46	97.74
Proposed (ANU-Net)	98.78	98.39	97.98	98.12

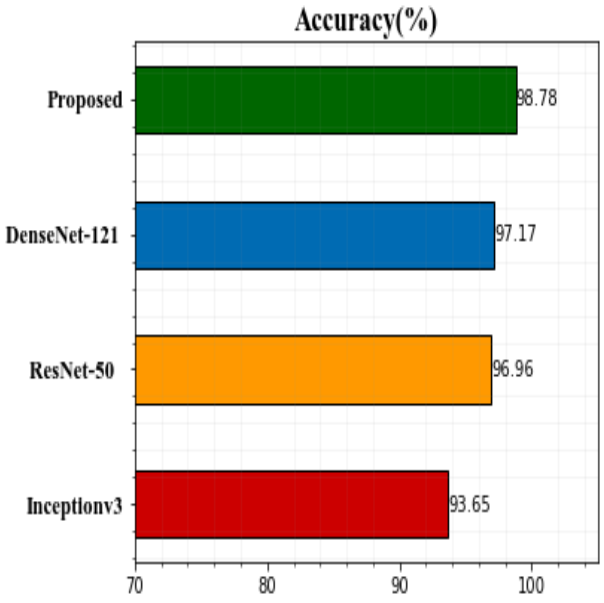

Fig. 6. Analysis of Accuracy based on different Techniques.

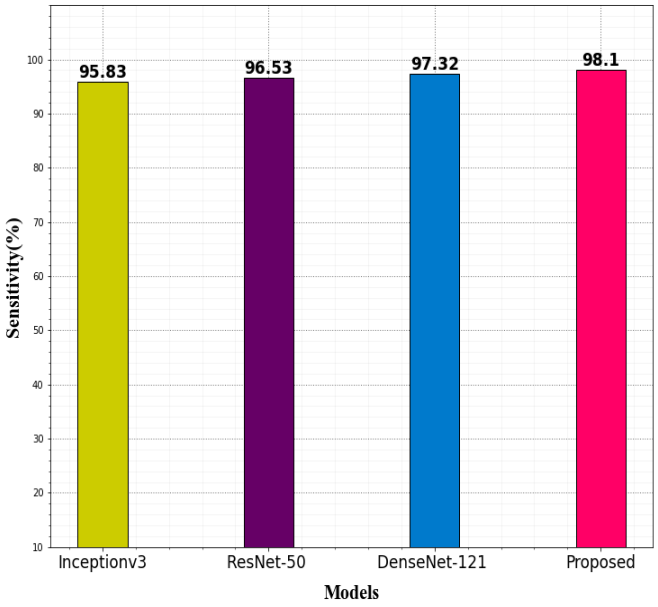

Fig. 7. Analysis of Sensitivity based on different Techniques.

The specificity metric achieved 97.98% using the proposed method ANU-Net technique compared with other techniques DenseNet-121 has 93.48%, ResNet-50 has 96.53%, and Inceptionsv3 has 96.46%. This sensitivity comparison model is shown in Fig. 8.

The precision metric achieved 98.12% using the proposed method ANU-Net technique compared with other techniques DenseNet-121 has 96.13%, ResNet-50 has 95.32%, and Inceptionsv3 has 97.74%. This sensitivity comparison model is shown in Fig. 9.

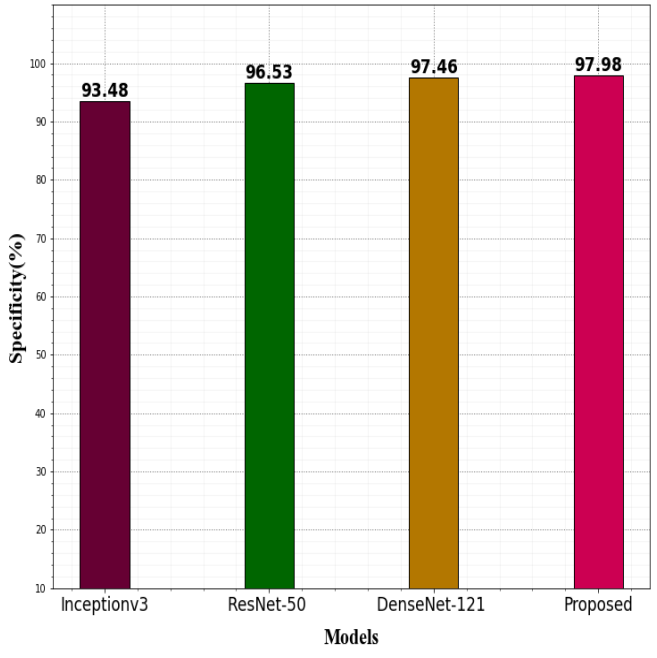

Fig. 8. Analysis of Specificity based on different Techniques.

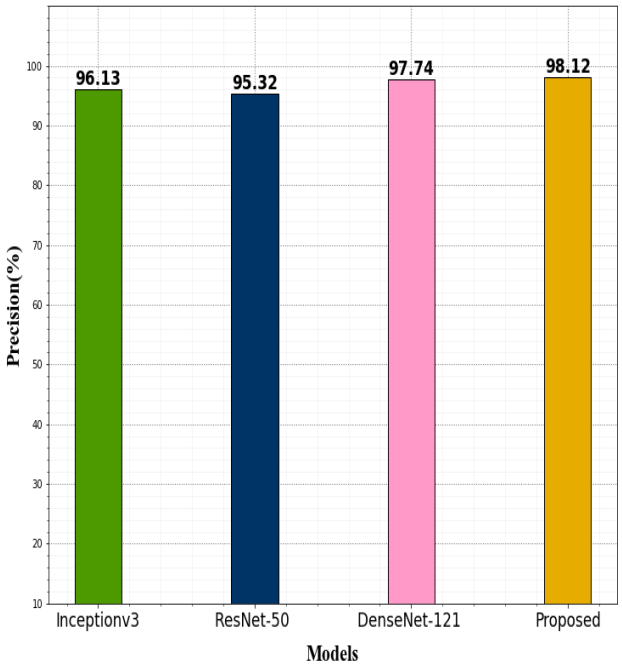

Fig. 9. Analysis of Precision based on different Techniques.

The analysis made by the different classification techniques is illustrated in the above figures. Compared with InceptionV3, ResNet-50, and DenseNet-121, the sensitivity value of ANU-Net is high and accurate the values are very clear and deep as shown in Fig. 7. And the same time also gives a better specificity percentage compared with other techniques as shown in Fig. 8. And also Fig. 9 shows the recall comparison of the ANU-Net technique.

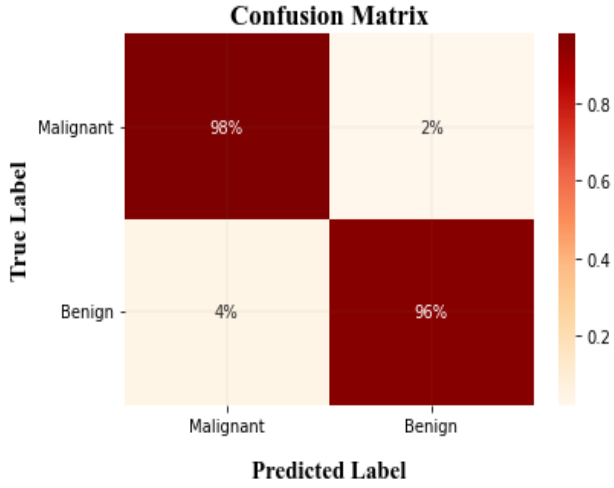

Fig. 10. Confusion Matrix of ANU-Net for Classification.

The confusion matrix is the most common tool for evaluating classification errors. Developed the confusion matrix for the ANU-Net proposed model based on the confusion matrix explanations offered. The graphic illustrates that the ANU-Net model can correctly categorize the two melanoma states (Malignant and Benign), with melanoma having a high ratio to malignant images and melanoma having

the lowest ratio to benign images. This indicates the classification of the two statuses has been completed appropriately. Fig. 10 presents the retrieved confusion matrix for the classification cross-validation test.

V. Conclusion and Future Works

Melanoma is the worst type of cancer among skin cancers, and its prevalence is rising globally. Early detection is crucial since skin cancer can be treated with a straightforward excision. But the mole's outline or outer covering is uneven, largely asymmetrical, and appears gritty. It states that around half of the moles present do not match the other half of the moles. To overcome all of this issues, proposed an effective methodology in this work. In this paper, the proposed system for melanoma classification involves four steps: Initially, pre-processing, removing hair from the dermoscopic images using a Laplacian-based algorithm, and then removing noise from the images using a Median filter. In addition, feature extraction from pre-processed images. Using the principal component analysis approach for extracting the characteristics like texture, shape, and color. These features for help to segment the skin lesion accurately from dermoscopic images. Furthermore, the segmentation process for identifying the lesion area and segmenting skin lesion using the LeNet-5 technique, and then, classification; categorizing lesion as benign (non-melanoma) and malignant (melanoma) using the ANU-Net method from the segmented skin lesion. It is classified into benign and malignant. The proposed technique solve these challenges in melanoma classification and given higher classification accuracy compared to other existing approaches. Therefore, based on the experimental findings, the ANU-Net method's accuracy for the ISIC2020 dataset is 98.78%. Since the ANU-Net model has the maximum level of accuracy, it can be effectively employed as a classifier to distinguish between malignant and benign skin lesions. It was established that the proposed model's categorization output was more accurate than that of the approaches under comparison. In the future, will work on new optimization techniques for better classification accuracy.

References

[1] Balasubramaniam, V. (2021). Artificial intelligence algorithm with SVM classification using dermoscopic images for melanoma diagnosis. Journal of Artificial Intelligence and Capsule Networks, 3(1), 34-42.

[2] Rehman, A., Khan, M. A., Mehmood, Z., Saba, T., Sardaraz, M., & Rashid, M. (2020). Microscopic melanoma detection and classification: A framework of pixel-based fusion and multilevel features reduction. Microscopy research and technique, 83(4), 410-423.

[3] Raza, R., Zulfiqar, F., Tariq, S., Anwar, G. B., Sargano, A. B., & Habib, Z. (2021). Melanoma classification from dermoscopy images using ensemble of convolutional neural networks. Mathematics, 10(1), 26.

[4] Damian, F. A., Moldovanu, S., Dey, N., Ashour, A. S., & Moraru, L. (2020). Feature selection of non-dermoscopic skin lesion images for nevus and melanoma classification. Computation, 8(2), 41.

[5] Thomas, S. M., Lefevre, J. G., Baxter, G., & Hamilton, N. A. (2021). Interpretable deep learning systems for multi-class segmentation and classification of non-melanoma skin cancer. Medical Image Analysis, 68, 101915.

[6] Almaraz-Damian, J. A., Ponomaryov, V., Sadovnychiy, S., & Castillejos-Fernandez, H. (2020). Melanoma and nevus skin lesion classification using handcraft and deep learning feature fusion via mutual information measures. Entropy, 22(4), 484.

[7] Maron, R. C., Utikal, J. S., Hekler, A., Hauschild, A., Sattler, E., Sondermann, W., ... & Brinker, T. J. (2020). Artificial intelligence and its effect on dermatologists' accuracy in dermoscopic melanoma image classification: web-based survey study. Journal of medical Internet research, 22(9), e18091.

[8] Pereira, P. M., Fonseca-Pinto, R., Paiva, R. P., Assuncao, P. A., Tavora, L. M., Thomaz, L. A., & Faria, S. M. (2020). Skin lesion classification enhancement using border-line features–The melanoma vs nevus problem. Biomedical Signal Processing and Control, 57, 101765.

[9] Roslin, S. E. (2020). Classification of melanoma from Dermoscopic data using machine learning techniques. Multimedia tools and applications, 79(5), 3713-3728.

[10] Dutta, A., Hasan, K., & Ahmad, M. (2021). Skin lesion classification using convolutional neural network for melanoma recognition. In Proceedings of International Joint Conference on Advances in Computational Intelligence (pp. 55-66). Springer, Singapore.

[11] Cheong, K. H., Tang, K. J. W., Zhao, X., Koh, J. E. W., Faust, O., Gururajan, R., ... & Acharya, U. R. (2021). An automated skin melanoma detection system with melanoma-index based on entropy features. Biocybernetics and Biomedical Engineering, 41(3), 997-1012.

[12] Cao, X., Pan, J. S., Wang, Z., Sun, Z., ul Haq, A., Deng, W., & Yang, S. (2021). Application of generated mask method based on Mask R-CNN in classification and detection of melanoma. Computer Methods and Programs in Biomedicine, 207, 106174.

[13] Gulati, S., & Bhogal, R. K. (2020). Classification of melanoma from dermoscopic images using machine learning. In Smart intelligent computing and applications (pp. 345-354). Springer, Singapore.

[14] Hosny, K. M., Kassem, M. A., & Foaud, M. M. (2020). Skin melanoma classification using ROI and data augmentation with deep convolutional neural networks. Multimedia Tools and Applications, 79(33), 24029-24055.

[15] Almaraz-Damian, J. A., Ponomaryov, V., Sadovnychiy, S., & Castillejos-Fernandez, H. (2020). Melanoma and nevus skin lesion classification using handcraft and deep learning feature fusion via mutual information measures. Entropy, 22(4), 484.

[16] Nawaz, M., Masood, M., Javed, A., Iqbal, J., Nazir, T., Mehmood, A., & Ashraf, R. (2021). Melanoma localization and classification through faster region-based convolutional neural network and SVM. Multimedia Tools and Applications, 80(19), 28953-28974.

[17] Cheong, K. H., Tang, K. J. W., Zhao, X., Koh, J. E. W., Faust, O., Gururajan, R., ... & Acharya, U. R. (2021). An automated skin melanoma detection system with melanoma-index based on entropy features. Biocybernetics and Biomedical Engineering, 41(3), 997-1012.

[18] Saxena, V. S., Johri, P., & Kumar, A. (2021). AI-Enabled Support System for Melanoma Detection and Classification. International Journal of Reliable and Quality E-Healthcare (IJRQEH), 10(4), 58-75.

[19] Rehman, A., Khan, M. A., Mehmood, Z., Saba, T., Sardaraz, M., & Rashid, M. (2020). Microscopic melanoma detection and classification: A framework of pixel-based fusion and multilevel features reduction. Microscopy research and technique, 83(4), 410-423.

[20] Li, C., Tan, Y., Chen, W., Luo, X., He, Y., Gao, Y., & Li, F. (2020). ANU-Net: Attention-based Nested U-Net to exploit full resolution features for medical image segmentation. Computers & Graphics, 90, 11-20.

[21] Fan, Y., Rui, X., Poslad, S., Zhang, G., Yu, T., Xu, X., & Song, X. (2020). A better way to monitor haze through image based upon the adjusted LeNet-5 CNN model. Signal, Image and Video Processing, 14(3), 455-463.